Information Storage

Role of Dipolar Interactions on the Thermal Stability of High-Density Bit-Patterned Media

Nasim Eibagi[1,2], Jimmy J. Kan[1,3], Frederick E. Spada[1], and Eric E. Fullerton[1,2,3]

[1] *Center for Magnetic Recording Research, University of California, San Diego, CA 92093, USA*
[2] *Electrical and Computer Engineering Department, University of California, San Diego, CA 92093, USA*
[3] *Materials Science and Engineering Department, University of California, San Diego, CA 92093, USA*

Received 20 June 2012, revised 16 July 2012, accepted 30 July 2012, published 31 August 2012.

Abstract—We have characterized the magnetic reversal and thermal stability of bit-patterned media with a composite structure of [Co (0.25 nm)/Pd (0.7 nm)]$_5$/Fe(X)/[Pd (0.7 nm)/Co (0.25 nm)]$_5$, where $X = 1$, 1.5, and 2 nm. For 25 nm diameter islands separated by 35 nm, the average thermal stability of the islands is confirmed by analyzing the time-dependent coercive fields. However, by further analyzing the time-dependent hysteresis loop shape, we find a broad distribution of the effective energy barriers. We quantitatively show that this energy barrier distribution arises primarily from the dipolar interactions in these densely packed arrays and not from intrinsic distributions.

Index Terms—Information storage, bit-patterned media, composite structures, dipolar interactions, energy barrier.

I. INTRODUCTION

Patterned magnetic structures are interesting due to their unique physics and their promising applications particularly for high-density magnetic information storage [Terris 2005, Engel 2005, Gallagher 2006]. Bit-patterned media (BPM) is a leading candidate to extend magnetic recording to densities beyond those achievable by perpendicular magnetic recording on continuous granular media [Moser 2002, Kikitsu 2007]. A key issue for exploiting patterned magnetic nanostructures is the ability to reproducibly make structures that are thermally stable, can be written at reasonable fields/currents, and exhibit uniform physical properties. For the implementation of BPM, the switching field distribution (SFD) (i.e., the bit-to-bit variation of the coercive field) has to be sufficiently narrow to secure addressability of individual bits.

The total SFD is due to both intrinsic and extrinsic contributions. The intrinsic part arises from local variation of individual island properties, which depend on the uniformity on the intrinsic material variations of the magnetic thin-film media [Terris 2005] but is also influenced by lithographic irregularities of the patterning process, such as island shape, size and spacing [Hellwig 2010]. The extrinsic contribution is the result of interactions between the islands. For patterned structures, where direct exchange is suppressed, the dominate interaction is expected to be dipolar (i.e., magneto-static interaction of an island with its neighbors) which for perpendicular anisotropy tends to broaden the total SFD [Berger 2005] and is also expected to broaden the distributions of the thermal stability parameters [Lubarda 2011a]. The extent to which interactions affect the SFD, thermal stability, and system performance, depends on the areal density, materials properties and the architecture of the media. In this paper, we quantify both the SFD and thermal stability distributions of high-density composite BPM. We further show that the dipolar interactions obtained from the SFD analysis quantitatively explains the thermal stability distributions.

II. EXPERIMENTAL PROCEDURE

The BPM samples were fabricated by patterning magnetic films of the structure Ta (2 nm)/[Co (0.25 nm)/Pd (0.7 nm)]$_5$/Fe (X)/[Pd (0.7 nm)/Co (0.25 nm)]$_5$/Pd (1 nm), where X has the value of 1, 1.5, or 2 nm. The films were grown by dc magnetron sputtering at 3-mTorr Ar pressure onto SiO_x coated Si wafers. We use the Fe layer thickness as a way to tune the anisotropy, coercive field and SFD of the BPM samples. By placing the Fe in the center of the stack, it is coupled at two surfaces and thus we have greater variability of Fe thickness while maintaining perpendicular remanence of the islands. This approach may further reduce the intrinsic SFD as it decoupled the reversal of the top and bottom multilayer structures. These samples are patterned using a self-assembling polymer as a mask with the magnetic film patterned by Ar ion milling as described in Kikitsu [2007] and Wang [2011]. This allows patterning large surface areas. Fig. 1 is a scanning electron microscope (SEM) image of the sample, which has an average dot diameter of 25 nm with a 35-nm pitch (corresponding to $\sim$0.5 Tbits/in^2). While there is no long-range order in the patterning, there is short-range hexagonal order that reflects the self-assembly process (see Fig. 1 inset). It is expected that the variations in the island size and spacing will contribute to the intrinsic SFD [Hellwig 2010].

We used vibrating sample magnetometer (VSM) and polar magneto-optic Kerr effect (P-MOKE) measurements to characterize the magnetic properties of the patterned arrays. We used minor loop measurements to quantify the intrinsic SFD and extrinsic interactions using the ΔH(M, ΔM) method [Berger 2005] and sweep-rate measurements to determine the energy barriers [Chantrell 1993].

Corresponding author: N. Eibagi (neibagi@gmail.com).
Digital Object Identifier: 10.1109/LMAG.2012.2211864

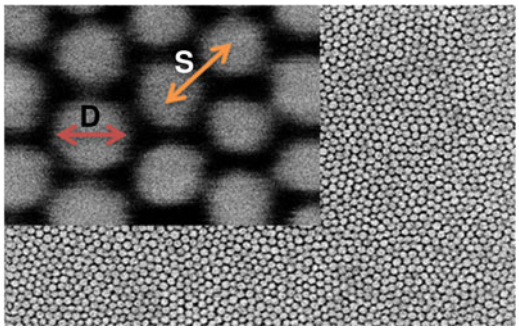

Fig. 1. SEM image of patterned islands which determines the average dot diameter of $D = 25$ nm and average spacing of $S = 35$ nm.

Table 1. Magnetic properties of patterned composite structure of $[Co/Pd]_5/Fe(X)/[Pd/Co]_5$ for three different Fe thickness.

Properties	Fe = 1nm	Fe= 1.5nm	Fe= 2nm
H_C (Oe)	3400	2400	1400
H_{C0} (Oe)	4650	3450	2330
σ_{total} (Oe)	1300	1330	1250
$\sigma_{intrinsic}$ (Oe)	365	265	205
$\sigma_{intrinsic}/H_{C0}$	7.8%	7.7%	8.8%
$E_B@H_C$ (k_B/T)	190	160	135
$H_d/(M/M_S)$ (Oe)	1235	1470	1495

The total (σ_{total}) and intrinsic ($\sigma_{intrinsic}$) SFDs and the ratio of the dipolar field H_d to M/MS were determined using the $\Delta H(M,\Delta M)$ method. Energy barriers (E_B) and short-time coercive fields (H_{C0}) were determined from timedependent coercive fields fitted to Eq. 1.

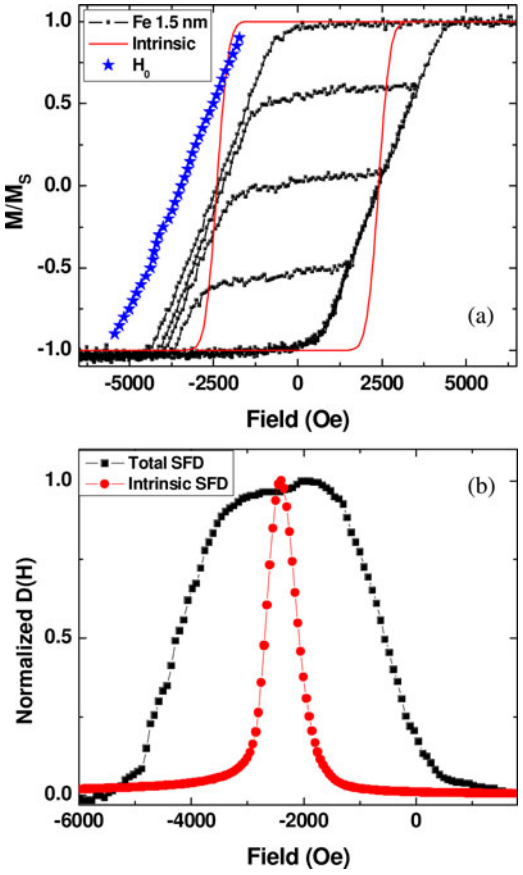

Fig. 2. (a) Out-of-plane major and minor loops for a $[Co/Pd]_5/Fe(1.5\ nm)/[Pd/Co]_5$ BPM sample measured by VSM (black points). The thin solid red line is the calculated intrinsic hysteresis corrected for the dipolar interactions, and the stars are the short-time-switching fields, H_0, for all values of M/M_s. (b) Results of the $\Delta H(M, \Delta M)$ method to separate the intrinsic distribution (circles) from the total SFD (squares).

III. RESULTS AND DISCUSSION

Fig. 2 shows the results of the out-of-plane magnetic measurements for the $X = 1.5$ nm sample. Table 1 further summarizes the results of the magnetization characterization for all the samples. The samples show high out-of-plane remanence, and coercive fields decrease with increasing Fe thickness (see Table 1). The major loop exhibits a broad transition during reversal, where a derivative of this loop gives the total SFD [see Fig. 2(b)]. The width of the total SFD, $\sigma_{(total)}$, is relatively insensitive to the Fe layer thicknesses as seen in Table 1. To separate the intrinsic $\sigma_{(intrinsic)}$ contributions to the total SFD, we used the $\Delta H(M, \Delta M)$ method to analyze the minor loops shown in Fig. 2(a) [Berger 2005]. This approach is an extension of the Tagawa and Nakamura [1991] approach which has been shown to be well suited for perpendicular recording media [Berger 2005] as well as patterned media [Hellwig 2007, Tudosa 2012] as long as interactions can be treated as a mean field. The functional form of the distribution that we used to fit the intrinsic distribution is the combination of two Gaussians

$$\sqrt{2}\sigma_1 \frac{erf^{-1}(M)}{(1+\alpha M)} + \sqrt{2}\sigma_2 \frac{erf^{-1}(M)}{(1+\beta M)}$$

where α and β are parameters that account for potential asymmetric shapes of the curves [Hellwig 2007]. Fig. 2(b) shows the extracted intrinsic distribution for $X = 1.5$ nm and compares it with the corresponding total SFD. The values for the width of the extracted distributions $\sigma_{(total)}$ and $\sigma_{(intrinsic)}$ for all three samples are given in Table 1. As the Fe thickness increases, the values of H_C and $\sigma_{(intrinsic)}$ decrease while $\sigma_{(total)}$ remains roughly constant at 1300 Oe. The fact that $\sigma_{(intrinsic)}$ is below $\sigma_{(total)}$ indicates antiferromagnetic interactions between the islands consistent with dipolar coupling. From the intrinsic distribution, we calculate the hysteresis loop in the absence of dipolar interactions, which is shown in Fig. 2(a), indicating a rather narrow intrinsic SFD. The difference between the intrinsic loop and the major loop is the average dipolar interaction.

To determine the island thermal stabilities and thermal stability distribution, the major hysteresis loops were measured using P-MOKE at four different magnetic field sweep rates R ranging from 4 to 4000 Oe/s. Plotted in Fig. 3 is the time dependence of the switching field at different M/M_S values. To extract the thermal stability parameters for the islands, the field sweep rate dependence of the switching field was fitted (see Fig. 3) using the Chantrell [1993] formula

$$H_s\left(\frac{M}{M_s}\right) = H_0\left(\frac{M}{M_s}\right)\left[1 - \left(\frac{1}{a}\ln\left(\frac{f_{0H_0}\left(\frac{M}{M_s}\right)}{2a}\frac{1}{R}\right)\right)^{\frac{1}{n}}\right] \quad (1)$$

where f_0 is the attempt frequency of about 10^{10} Hz, the expo-

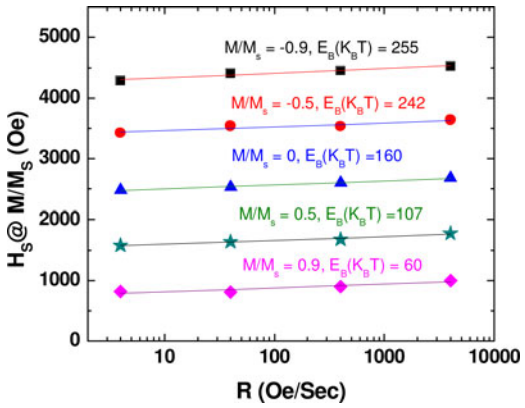

Fig. 3. Time-dependent switching fields for a $[Co/Pd]_5/Fe(1.5\ nm)/[Pd/Co]_5$ BPM sample at selected M/M_S values. The solid lines are fit to (1) yielding an effective energy barrier and short-time switching field. The result for the short-time switching field is shown in Fig. 2(a), and the energy barriers for all M/M_S values are shown in Fig. 4.

nent $n = 3/2$ is used to account for possible incoherent reversal processes that arise from the Fe layers [Bertram 2007], R is the magnetic field sweep rate, $H_S(M/M_S)$ and $H_0(M/M_S)$ are the switching field and the short-time switching field at the given M/M_S value, respectively, and $a = E_B(M/M_S)/k_BT$ is the ratio of energy barrier to thermal energy for the islands switching at a given M/M_s. The results for $E_B(M/M_S = 0) = K_uV$ (the average island stability) and H_{C0}, extracted from the sweep-rate-dependent coercive fields are given in Table 1. The H_{C0} values like H_C decreases as Fe thickness increases and this is due to the reduction in the effective anisotropy of the system as the thickness of the soft Fe layer increases. The intrinsic SFD as a ratio of H_0 is relatively constant as was recently seen in composite [Co/Pd]-[Co-Ni]-based BPM [Hellwig 2009]. The average value of the energy barrier for the islands scales like H_0, with the average energy barrier still stable for 2-nm Fe layers.

In addition to extracting the value of the average energy barrier measured at H_C, we apply (1) to extract both H_0 and E_B for various values of M/M_S. Shown in Fig. 2 are the switching fields for selected M/M_S values for the descending branch of the hysteresis loop ($M/M_S = 0$ corresponds to H_C). As M/M_S decreases from 0.9 to –0.9, the switching fields increase, simply reflecting the sheared hysteresis loop, in Fig. 2(a). The values for H_0 for all M/M_S values are shown in Fig. 2(a) which is the expected loop shape for fast times switching in the absence of thermal excitations. Also shown in Fig. 3 are $E_B(M/M_S)$, the energy barrier for island reversing at a given M/M_S, which increases dramatically with decreasing M/M_S. That is, the first islands to reverse (near $M/M_S = 1$) have a much lower effective E_B compared to the last islands to reverse. This trend can have two basic origins. The first is intrinsic, where the islands with the lowest anisotropy and/or volume, and hence lowest E_B, switch first. The second arises from interactions via the dipolar fields. For positive M/M_S, the dipolar fields aid reversal and therefore lower the effective E_B. For negative M/M_S, the dipolar interactions oppose reversal and raise E_B.

Fig. 4 shows the distribution of E_B measured for the three samples as a function of M/M_S. As can be seen, there is a broad

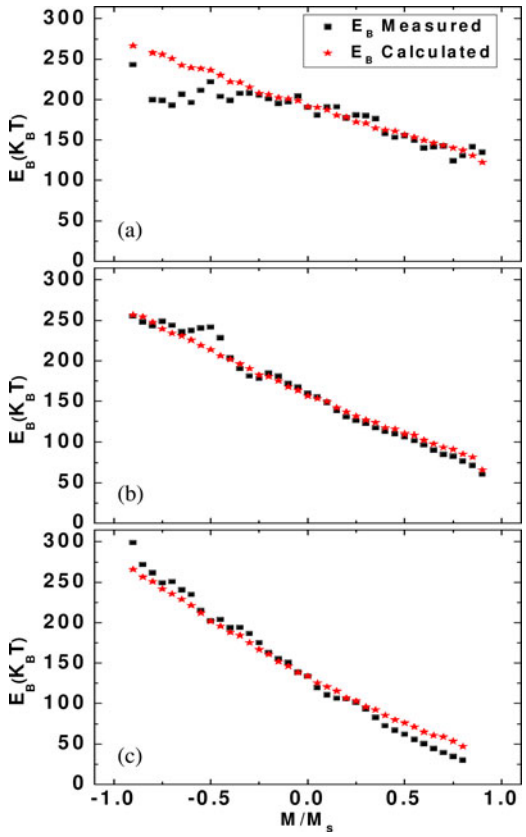

Fig. 4. The distribution of energy barriers for $[Co/Pd]_5/Fe(X)/[Co/Pd]_5$ BPM samples: (a) $X = 1.0$ nm, (b) $X = 1.5$ nm, and (c) $X = 2.0$ nm. The squares show the measured values of E_B for each M/M_S value that is determined from time-dependent hysteresis loops. The stars are the calculated values (2) assuming no intrinsic distribution in E_B.

range of E_B values and this range increases with increasing Fe thickness. For 1-nm Fe layers, the E_B ranges from 150 to 250 k_BT, while for 2-nm Fe this range increases to 20 to 300 k_BT more than an order of magnitude distribution in values of E_B for the range of M/M_S values.

To quantify the role of the dipolar fields on the energy barrier distribution E_B, we need the average dipolar field at each M/M_S value given by $H_d(M/M_S)$. This distribution can be extracted from the field difference of the intrinsic loop and the measured hysteresis loop in Fig. 2(a) at each M/M_S. As might be expected for a mean-field interaction, H_d is roughly linear with M/M_S. We give the ratio of $H_d/(M/M_S)$ in Table 1 which increases with increasing Fe thickness. Given $H_d(M/M_S)$, we can estimate E_B for all M/M_S relative to the mean value $E_B(0)$ (see Table 1) using the Stoner–Wohlfarth model

$$E_B\left(\frac{M}{M_s}\right) = E_B(0)\left[1 - \left(\frac{H_d\left(\frac{M}{M_s}\right)}{H_{co}}\right)\right]^n \qquad (2)$$

where we use the exponent $n = 3/2$ in correlation with (1).

Applying (2), we calculate the expected E_B distributions in Fig. 4 assuming no intrinsic E_B distributions. As can be seen, these calculations quantitatively agree with the measured values showing that the origin of the distribution is driven

primarily by dipolar interactions, at least for the dense packed BPM with modest coercive fields studied here. Any intrinsic distribution in E_B is small as compared to the distributions arising from the dipolar interactions. We should note that this agreement does not depend on the specific choice of the exponent n in (1) and (2) as long as the same n value is used in both equations. While the quantitative values for H_0 and E_B do vary by varying n, the calculated and measured energy barrier distributions are self-consistent.

The results in Fig. 4 show that the dipolar interactions can have a dramatic impact on the thermal stability of patterned media particularly for high-density patterns and relatively modest coercive fields. This may place limits on the coercive field for BPM in relation to the dipolar fields or will require media designs that limit the dipolar interactions. Examples include antiferromagnetically coupled BPM [Ranjbar 2010] or capped BPM, where a continuous capping layer is coupled to the BPM [Lubarda 2011a, 2011b]. Micromagnetic models have shown that the exchange interactions introduced through coupling with a continuous capping layer can effectively offset the energy barrier distribution arising from dipolar interactions.

IV. CONCLUSION

We have studied the magnetic properties of patterned islands with a composite [Co/Pd]/Fe/[Pd/Co] multilayer structure. By tuning the Fe thickness, we could tune the coercive field while maintaining a narrow intrinsic SFD. The total SFD was relatively independent of the Fe thickness. It was determined that dipolar interactions mainly contribute to the broadening of SFD. We extracted the thermal stability parameters for all values of magnetization and show that while the average energy barrier may be stable, dipolar interactions can result in large distributions in the effective energy barriers.

ACKNOWLEDGMENT

We would like to acknowledge financial support of the sponsors of the Center for Magnetic Recording Research. N. Eibagi and E. E. Fullerton were partially supported by DOE-BES Award DE-SC0003678. We gratefully acknowledge collaborations with the Toshiba R&D Center on this research.

REFERENCES

Berger A, Xu Y, Ikeda Y, Fullerton E E (2005), "ΔH(M, ΔM) method for the determination of intrinsic switching field distributions in perpendicular media," *IEEE Trans. Magn.*, vol. 41, no. 10, pp. 3178–3180, doi: 10.1109/TMAG.2005.855285.

Bertram H N, Lengsfield B (2007), "Energy barriers in composite media grains," *IEEE Trans. Magn.*, vol. 43, no. 6, pp. 2145–2147, doi: 10.1109/TMAG.2007.892852.

De Witte A M, El-Hilo M, O'Grady K, Chantrell R W (1993), "Sweep rate measurements of coercivity in particulate recording media," *J. Magn. Magn. Mater.*, vol. 120, pp. 184–186, doi: 10.1016/0304-8853(93)91316-Y.

Engel B N, Akerman J, Butcher B, Dave R W, DeHerrera M, Durlam M, Grynkewich G, Janesky J, Pietambaram S V, Rizzo N D, Slaughter J M, Smith K, Sun J J, Tehrani S (2005), "A 4-Mb toggle MRAM based on a novel bit and switching method," *IEEE Trans. Magn.*, vol. 41, no. 1, pp. 132–136, doi: 10.1109/TMAG.2004.840847.

Gallagher W, Parkin S S P (2006), "Development of the magnetic tunnel junction MRAM at IBM: from first junctions to a 16-Mb MRAM demonstrator chip," *IBM J. Res. and Dev.*, vol. 50, pp. 5–23, doi: 10.1147/rd.501.0005.

Hellwig O, Berger A, Thomson T, Dobisz E, Bandic Z, Yang H, Kercher D S, Fullerton E E (2007), "Separating dipolar broadening from the intrinsic switching field distribution in perpendicular patterned media," *Appl. Phys. Lett.*, vol. 90, 162516, doi: 10.1063/1.2730744.

Hellwig O, Hauet T, Thomson T, Risner-Jamtgaard E J D, Yaney D, Terri B D, Fullerton E E (2009), "Coercivity tuning in Co/Pd multilayer based bit patterned media," *Appl. Phys. Lett.*, vol. 90, 232505, doi: 10.1063/1.3271679.

Hellwig O, Bosworth J K, Dobisz E, Kercher D, Hauet T, Zeltzer G, Risner-Jamtgaard J D, Yaney D, Ruiz R (2010), "Bit Patterned media based on block copolymer directed assembly with narrow magntic switching field distribution," *Appl. Phys. Lett.*, vol. 96, 052511, doi: 10.1063/1.3293301.

Kikitsu A, Kamata Y, Sakurai M, Naito K (2007), "Recent progress of patterned media," *IEEE Trans. Magn.*, vol. 43, no. 9, pp. 3685–3688, doi: 10.1109/TMAG.2007.902970.

Lubarda M V, Li S, Livhitz B, Fullerton E E, Lomakin V (2011a), "Reversal in bit patterned media with vertical and lateral exchange," *IEEE Trans. Magn.*, vol. 47, no. 1, pp. 18–25, doi: 10.1109/TMAG.2010.2089610.

Lubarda M V, Li S, Livhitz B, Fullerton E E, Lomakin V (2011b), "Antiferromagnetically coupled capped bit patterned media for high density magnetic recording," *Appl. Phys. Lett.*, vol. 98, 012513, doi: 10.1063/1.3532839.

Moser A, Takano K, Margulies D T, Albercht M, Sonobe Y, Ikeda Y, Sun S H, Fullerton E E (2002), "Magnetic recording: advancing into the future," *J. Phys. D: Appl. Phys.*, vol. 35, pp. R157–R167, doi: 10.1088/0022-3727/35/19/201.

Ranjbar M, Piramanayagam S N, Deng S Z, Aung K O, Sbiaa R, Wong S K, Chong C T (2010), "Antiferromagnetically Coupled Patterned Media and Control of Switching Field Distribution," *IEEE Trans. Magn.*, vol. 46, no. 6, pp. 1787–1790, doi: 10.1109/TMAG.2010.2043226.

Tagawa I, Nakamura Y (1991), "Relationships between high density recording performance and particle coercivity distribution," *IEEE Trans. Magn.*, vol. 27, pp. 4975–4977, doi: 10.1109/20.278712.

Terris B D, Thomson T (2005), "Nanofabricated and self-assembled magnetic structures as data storage media," *J. Phys. D: Appl. Phys.*, vol. 38, pp. R199–R222, doi: 10.1088/0022-3727/38/12/R01.

Tudosa I, Lubarda M V, Chan K T, Escobar M A, Lomakin V, Fullerton E E (2012), "Thermal stability of patterned Co/Pd nanodot arrays," *Appl. Phys. Lett.*, vol. 100, 102401, doi: 10.1063/1.3692574.

Wang H, Rahman M T, Zhao H, Isowaki Y, Kamata Y, Kikitsu A, Wang J (2011), "Fabrication of FePt type exchange coupled composite bit-patterned media by block copolymer lithography," *J. Appl. Phys.*, vol. 109, 07B754, doi: 10.1063/1.3562453.